

Response to Anonymous Referee #1

Discussion Paper wes-2016-37

Effect of the Foundation Modelling on the Fatigue Lifetime of a Monopile-based Offshore Wind Turbine

Steffen Aasen, Ana Page, Kristoffer Skjolden Skau, and Tor Anders Nygaard

Dear reviewer,

We would like to thank you for spending time and effort in reviewing our paper. Your comments are much appreciated. We have replied to each of them in the text below and specified which actions will be taken in the paper.

Best regards,

Steffen Aasen, Ana Page, Kristoffer Skjolden Skau, and Tor Anders Nygaard

1. Introduction

a) A paragraph reviewing methods used for modelling soil-solid interactions, such as p-y curve method and 3D (three-dimensional) FEA (finite element analysis) method, should be added.

We will include a paragraph reviewing the methods used for soil-solid interaction in the introduction after line 18. Our suggestion reads as follows:

“Different approaches can be used to model the soil-foundation response for piles. Generally, they are divided into two groups: continuum approaches and subgrade reaction approaches. In continuum approaches, the soil is treated as a continuum material described by a constitutive relation. The problem of a pile embedded in a continuum material can be solved analytically if the soil is assumed to be a linear-elastic material (e.g. Poulos (1971)) or numerically if the soil is characterized by a more complex constitutive relation. Among the numerical methods, the boundary element method (e.g. Kaynia and Kausel (1982)) and the finite element method (e.g. Randolph (1981) or Andresen et al. (2010)) are the most widely used. In the subgrade reaction approaches, the soil response around the pile is described by a set of uncoupled individual horizontal springs, where the interaction between layers is only taken into account by the pile continuity. The springs relate the local lateral resistance, p , to the local lateral displacement of the pile, y , following a predefined function. Several p - y functions can be found in the literature (e.g. Reese and Van Impe (2010)), however, the API (API 2011) p - y curves are the most widely used.”

b) A review on relevant studies, such as fatigue assessment of OWT (offshore wind turbine monopile), should be added.

A short note on fatigue assessment for offshore wind turbines (OWT's) will be added in the introduction as follows:

“The most widespread methods for fatigue estimations are time domain simulations with S-N curves and frequency domain calculations. A comparison of these methods can be found in Ragan and Manuel (2007). The industry standard for fatigue damage calculations is the time domain simulations with S-N curves described by DNV (Det Norske Veritas 2014). This methodology is used in this article.»

More references will be added in section 4.5 for details on spectral methods:

“Fatigue damage can be evaluated in both time- and frequency domain. For time domain simulations, the S-N curve methodology is widely used, and is briefly described below. Frequency domain simulations can also be performed using Dirluk's method (Dirluk 1985). A comparison between these methods can be found in Ragan and Manuel (2007). More details on spectral methods for fatigue assessment can be found in Yeter et al. (2013) and Michalopoulos (2015)».

c) It would be appropriate to present the outline of the paper at the end of the introductory section, making the structure of the paper clear.

We agree with the reviewer's suggestion and will add a paragraph at the end of the introductory section as follows:

“Following the introduction, Chapter 2 gives a review of observed foundation behavior, current foundation models for OWT monopiles, and relevant studies investigating effects of soil stiffness and damping. Chapter 3 presents the simulation software 3DFloat and the different soil-

foundation models studied in this paper. Chapter 4 presents the OWT structure, the soil profile and the environmental conditions that has been applied in simulations. The calibration of each soil-foundation model, together with our methodology for fatigue damage calculations is also included at the end of Chapter 4. Chapter 5 presents the results from the analysis that has been carried out, followed by a conclusion with suggestions for further work in Chapter 6.”

2. Section 3.1

Please give more details about how the wind and wave loads were applied on the monopile. Were they applied as point load or distributed load?

The wind and wave loads are distributed on the structure. Forces per unit length are integrated with the interpolation functions used in the Galerkin formulation of the Finite-Element-Method. The distributed forces are thereby lumped to consistent nodal loads (forces and moments), applied to the nodes connecting the elements. The forces on the wet elements of the pile below the instantaneous wave surface are computed with Morison's equation. The quadratic drag forces on the tower above the instantaneous wave surface are computed from the turbulent wind. The wind turbine distributed blade loads are computed from Blade Element Momentum theory, taking into account the elastic deformation of the structure.

We will merge this information into section 3.1.

3. Section 4.1

Please give the thickness of the monopile used in this study.

We have modified 'Figure 9: Soil profile and pile dimensions' to include it, as shown in Figure 1.

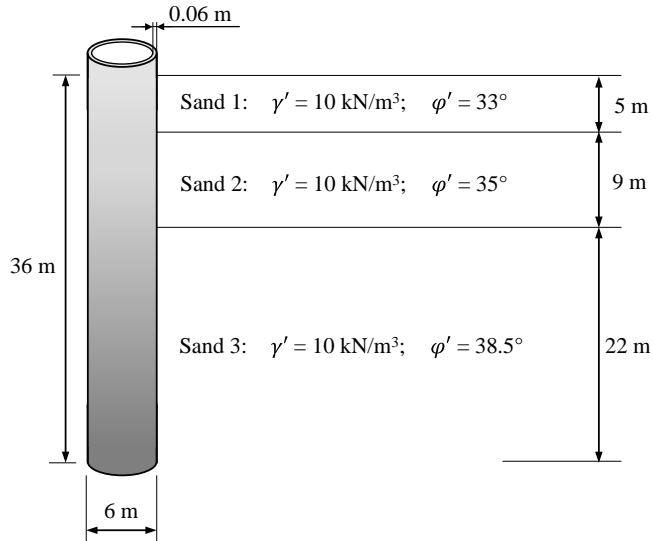


Figure 1: Soil profile and pile dimensions

4. Section 4.2

For soil profile, please present the p-y curves for three types of sands used in this study, i.e. loose, medium and dense sands.

Following the reviewer's suggestion, we have plotted three p - y curves, one for each of the soil layers considered in this study. The blue curve at $z = 2 \text{ m}$ is representative for the top soil layer,

which extends from seabed to $z = 5$ m; the green curve is representative for the middle layer, which extends from $z = 5$ m to $z = 14$ m; and the red curve is representative for the bottom sand layer, which starts from $z = 14$ m. The vertical axis is normalized by the depth of the p - y curve considered.

This figure will be included in section 4.4.4., where the calibration of the p - y curves for the soil profile considered is presented.

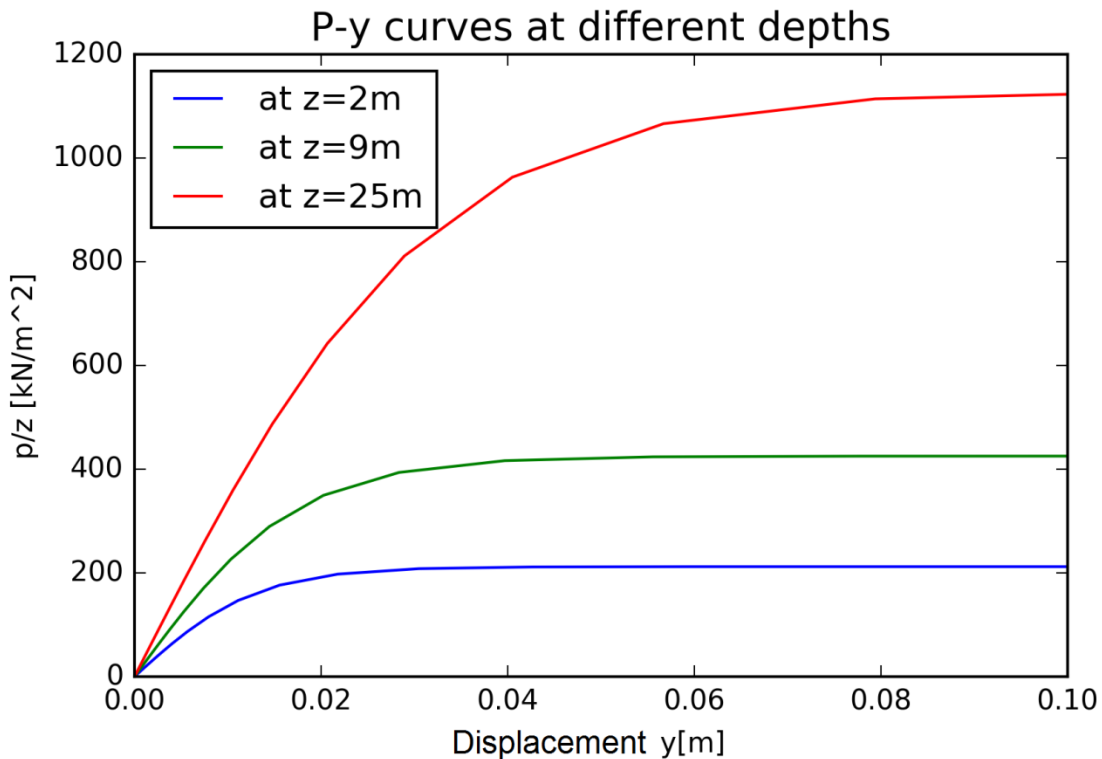


Figure 2: Representative p - y curves of each of the soil layers considered in this study. The vertical axis is normalized by the depth at which the p - y curve is calculated.

5. Section 4.3

Please present some load calculation results of both wind and wave loads, e.g. the load calculation results for Load Cases 5 and 6.

We will include detailed results for the load cases (LC) 5, 6 and 1 (idle). LC 1 will be included to examine the significant contribution to fatigue, despite the mild wind and wave conditions for this case.

Figure 3 gives the tower top force in the wind direction, representing forces from the wind turbine (with inertial forces). Additional simulations must be run to extract wave forces, and will be included in the revised version of the paper.

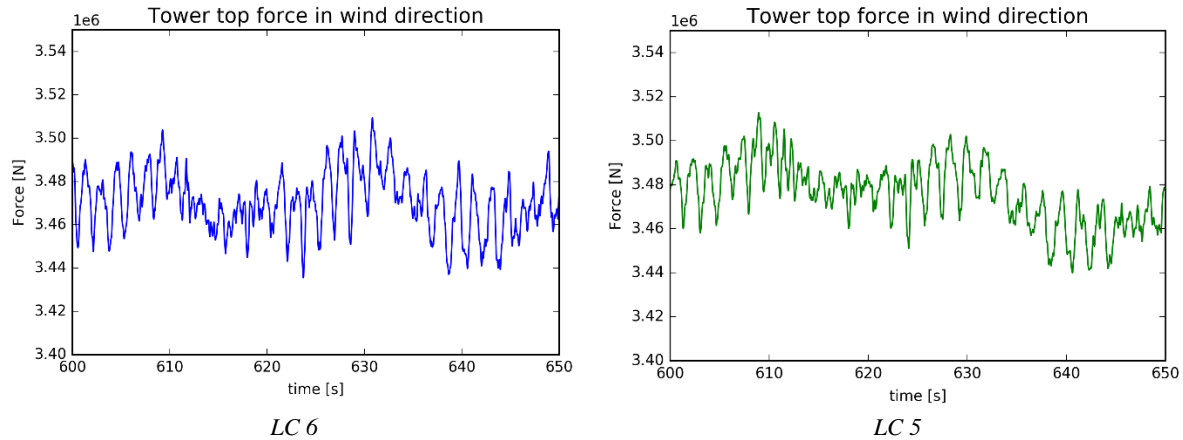


Figure 3: Tower top force along x-axis (in wind direction)

6. Section 4.4.3

Please give more details about the FE model, such as types of elements, mesh size, displacement boundary conditions, the amplitude of the horizontal load H, and contact type between the soil and pile. Were mesh sensitivity exercises performed?

Thank you for this comment, this information should have been included in the text.

The commercial finite element software PLAXIS 3D AE was used to perform the analyses with 10-noded tetrahedral elements. Table 1 lists the model dimensions based on the axis shown in Figure 4. Only half of the pile and the soil volume were modelled since both the geometry and the load acting on the pile are symmetric. A horizontal load of 1.955 MN was applied to half of the FE-model. This horizontal load is the same one used by Passon (2006) to calibrate the elastic stiffness matrix at seabed in Phase II of the comparison exercise OC3 (Jonkman and Musial 2010).

Table 1 Finite Element model dimensions

x_{max}	x_{min}	y_{max}	y_{min}	z_{max}	z_{min}
m	m	m	m	m	m
63	-63	42	0	0	-50

The displacements at bottom boundary (z_{min}) are fixed, while roller boundaries are applied on the model sides (x_{max} , x_{min} , y_{max} , y_{min}). The mesh has 45 711 soil elements and 66 868 nodes. The average element size of the whole model is about 3 m, but significantly refined around the pile (approximately 1.3m). Figure 4 shows the mesh discretization.

Full contact was assumed between the pile and the soil.

Yes, a mesh sensitivity study was performed to assure that the mesh discretization was enough. In the mesh sensitivity study, two mesh discretization were compared:

1. The mesh discretization used in the paper, with 45 711 elements and 66 868 nodes, shown in Figure 4.
2. The finest mesh discretization that was possible to achieve in PLAXIS 3D, with 907 570 elements and 1 238 593 nodes, shown in Figure 5.

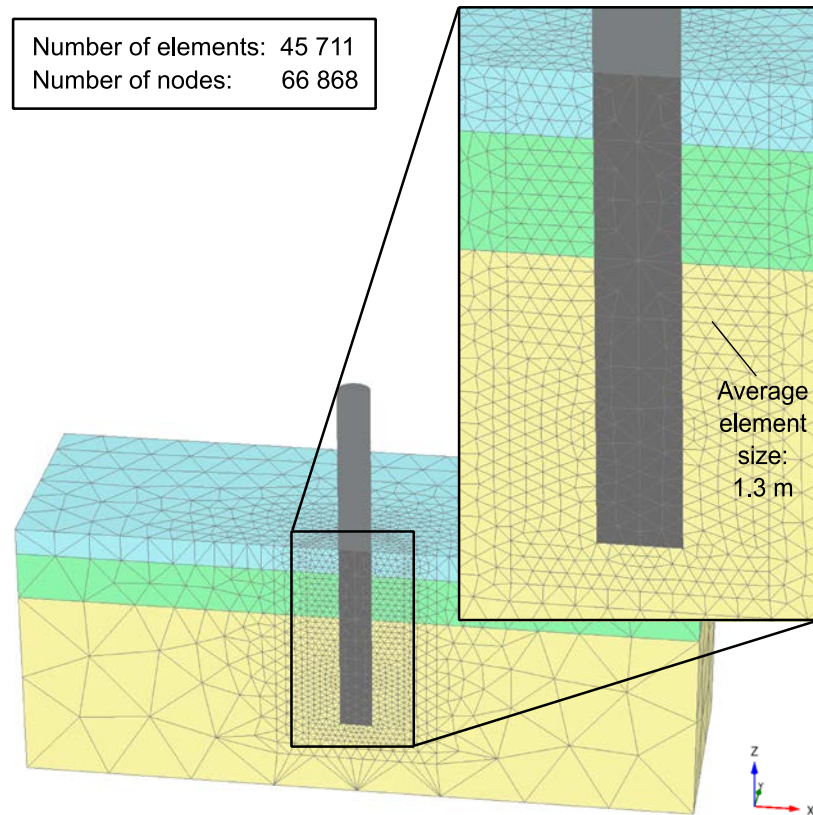


Figure 4: Mesh of the finite element model

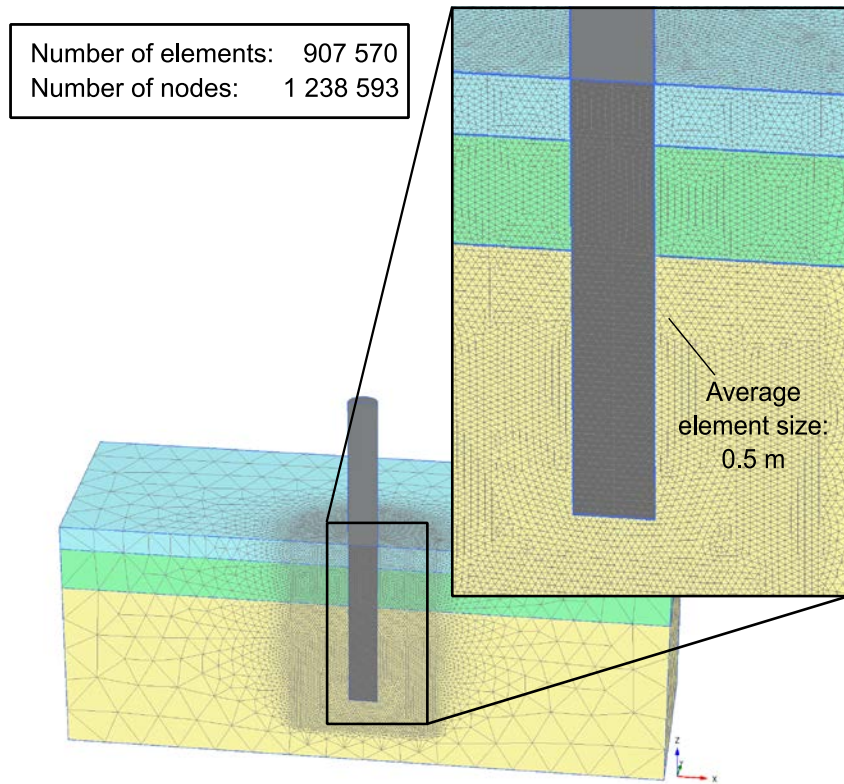


Figure 5: Mesh discretization used in the mesh sensitivity study

The horizontal load – horizontal displacement curves at seabed calculated with the two mesh discretizations are compared in Figure 6. The almost perfect coincidence between the two curves demonstrates that the discretization in the paper is sufficient.

The figures showing the comparison will not be included in the paper. However, we will include in page 14 around line 6:

"The horizontal load – horizontal displacement curve at seabed was compared with a FE-model with significantly refined mesh and the discretization error shown to be less than 1 % for the load range considered in the study."

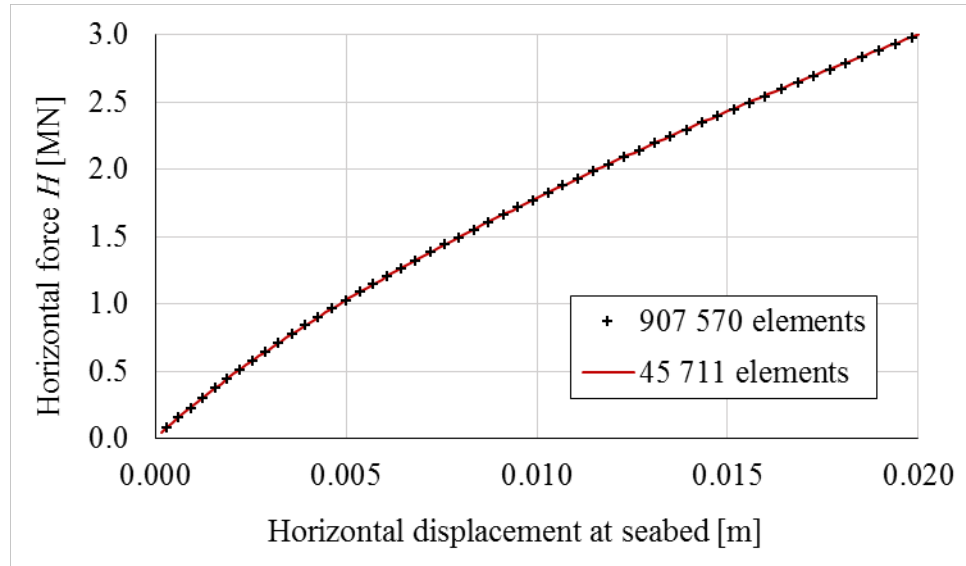


Figure 6: Horizontal load – horizontal displacement curves at seabed calculated with the two mesh discretizations

7. Section 4.5

Please justify why DNV F3 in-air S-N curve was chosen in this study. Please give details how the wind and wave load period were determined for the fatigue analysis.

Thank you for noticing this. The DNV F3 in-air S-N curve was chosen for simplicity. New calculations will be done at the mudline by using "DNV F3 in seawater with cathodic protection", as this position is exposed to seawater. This is the recommended S-N curve in DNV OS-J101 for tubular girth welds (Det Norske Veritas 2014).

Wind and wave periods are chosen from the Upwind Design Basis (Fischer et al. 2010), giving a lumped scatter diagram for wind and waves. The lumped scatter diagram should represent a possible shallow water site for monopile installation in the Dutch North Sea. This is further explained in section 4.3 of the paper. The lumping has been done according to methodology described by Kühn (2001).

8. Section 5.3

According to Figs. 17 and 19, LC1 (load case 1) has a high impact on the total fatigue damage. This seems unreasonable, as the both wind and wave loads are relatively low. Authors state “with little aerodynamic damping, the tower is free to oscillate at its first

natural frequency, leading to high load amplitudes at the mudline". Can authors compare the load calculation results for LC1 obtained from 3Dfloat against the results obtained from other aero-hydro-elastic codes, e.g. NREL FAST, to confirm this?

We think it is a good idea to examine this case closer. It is well known that the idle cases contribute significantly to fatigue damage for monopiles due to the low damping when the rotor is idle. The results are, however, sensitive to structural damping, the damping in the soil, the excitation around the tower eigen frequency, the damping inherent in the hydrodynamic and aerodynamic load models, and the nonlinearities and frequency content of the excitation from the quadratic drag models. We have neglected hydrodynamic radiation damping so far based on the literature review, but this can be included in the revised paper. The OC3 monopile has been studied with FAST and several other models in the IEA OC3 project, and we are going to invite colleagues to revisit the OC3 monopile for LC 1, 5 and 6.

References

Andresen, L., H. Petter Jostad and K. H. Andersen (2010). "Finite element analyses applied in design of foundations and anchors for offshore structures." *International Journal of Geomechanics* **11**(6): 417-430.

API (2011). Recommended Practice for Planning, Designing and Constructing Fixed Offshore Platforms - Working Stress Design, American Petroleum Institute.

Det Norske Veritas (2014). Design of offshore wind turbine structures, Det Norske Veritas: 238.

Dirlik, T. (1985). *Application of computers in fatigue analysis*, University of Warwick.

Fischer, T., W. De Vries and B. Schmidt (2010). UpWind Design Basis (WP4: Offshore foundations and support structures), Upwind.

Jonkman, J. and W. Musial (2010). Offshore code comparison collaboration (OC3) for IEA task 23 offshore wind technology and deployment: 275-3000.

Kaynia, A. and E. Kausel (1982). *Dynamic behavior of pile groups*. 2nd Int. Conf. on Numerical Methods in Offshore Piling, Austin, Texas.

Kühn, M. J. (2001). *Dynamics and design optimisation of offshore wind energy conversion systems*, TU Delft, Delft University of Technology.

Michalopoulos, M. (2015). *Simplified fatigue assessment of offshore wind support structures accounting for variations in a farm*, EWEA European Wind Energy Association.

Passon, P. (2006). "Memorandum: derivation and description of the soil-pile-interaction models." *IEA-Annex XXIIII Subtask 2*.

Poulos, H. G. (1971). "Behavior of Laterally Loaded Piles: I-Single Piles." *Journal of the Soil Mechanics and Foundations Division* **97**(5): 711-731.

Ragan, P. and L. Manuel (2007). "Comparing estimates of wind turbine fatigue loads using time-domain and spectral methods." *Wind engineering* **31**(2): 83-99.

Randolph, M. F. (1981). "The response of flexible piles to lateral loading." *Geotechnique* **31**(2): 247-259.

Reese, L. C. and W. F. Van Impe (2010). *Single piles and pile groups under lateral loading*, CRC Press.

Yeter, B., Y. Garbatov and C. G. Soares (2013). "Spectral fatigue assessment of an offshore wind turbine structure under wave and wind loading." *Developments in Maritime Transportation and Exploitation of Sea Resources*: 425-433.